Abridged version

KAWASAKI STEEL TECHNICAL REPORT
No.2 (March 1981)

Interlock Strength of Flat-type Steel Sheet Piling

Teruyuki Nakanishi, Takafumi Hashimoto, Katsumi Shibata, Hidetoshi Takeda, Hironori Miura

Synopsis :
Experimental and theoretical studies have been carried out on the interlock strength of flat-type sheet piling. Factors such as dimensions of interlocking part, mechanical properties of the steel and coefficient of friction have been examined to clarify their effect on the interlock strength. Also, sheet piling with interlock strength expected over 700 t/m and ease of driving has been designed by lowering axial load distribution to finger.

The body can be viewed from the next page.

KAWASAKI STEEL TECHNICAL REPORT No. 2 March 1981

Interlock Strength of Flat-type Steel Sheet Piling*

Teruyuki NAKANISHI ** Takafumi HASHIMOTO ** Katsumi SHIBATA **
Hidetoshi TAKEDA *** Hironori MIURA **

Experimental and theoretical studies have been carried out on the interlock strength of flat-type sheet piling. Factors such as dimensions of interlocking part, mechanical properties of the steel and coefficient of friction have been examined to clarify their effect on the interlock strength. Also, sheet piling with interlock strength expected over 700 t/m and ease of driving has been designed by lowering axial load distribution to finger.

1 Introduction

Cell structures using flat-type steel sheet pilings were first adopted in Japan in 1954 in the construction of a quay for 10 000 t vessels at Shiogama harbor, and they have since been employed in large numbers, triggered by the development of a new method of execution[1]. Kawasaki Steel Corporation commenced the production of KSP-F with web thickness 9.5 mm, and achieved a number of executions. Recently, owing to the growing scale of construction and product design for corrosion resistance, demand is increasing for the so-called FA type of web thickness 12.7 mm.

In constructing a cell structure, flat-type steel sheet pilings are driven into the ground to form a circle or circular arc and earth is cased into the circle so as to resist the earth or water pressure from behind[2]. The flat-type steel sheet piling used in this work is subjected to a great tensile force in parallel to the web. This structure may be regarded as effective in utilizing the features of steel materials to a high degree.

Among the characteristics of flat-type steel sheet piling, the tensile strength of interlock is most important. In order to utilize the tensile strength of steel material fully, the interlock part should be designed so that separation at interlock does not occur before the rupture of the web. This is especially important in case of FA type piling with thicker web. The authors developed FA flat-type steel sheet piling after determing an optimal form of interlock to increase the interlock strength through analysis based on a theoretical calculation and experiment with tensile test of interlock. An outline of this study will be presented below.

* Originally published in *Kawasaki Steel Technical Report* **11**(1979) 4, pp. 97–109 (in Japanese)
** Mizushima Works
*** Tubarão Project Division

2 Characteristics Required for Flat-type Steel Sheet Pilings

Flat-type steel sheet pilings are required to have the following characteristics:

(1) High interlock strength
(2) Good workability
(3) Excellent water-tightness capability

Since the interlocks of pilings are used in the state of rigid contact under high tensile force, the water-tightness capability is not so much affected by the geometry of the interlock. The workability is said to be better if the maximum revolution angle of interlocked pilings is greater, and the maximum revolution angle depends upon the geometry of interlock. In case of flat-type steel sheet piling, it is necessary to ensure stable and high interlock strength, to improve the reliability of cell strength. The maximum revolution angle of interlocked pilings is qualitatively related to the interlock strength, as shown in **Fig. 1**; the greater the interlock strength is, the smaller the maximum revolution angle becomes. Flat-type steel sheet piling is, therefore, required to meet conflicting requirements for good workability and adequate interlock strength.

The principal aim of developing FA type piling was placed on the determining the interlock shape which minimizes the weight increment and increases the interlock strength without reducing the maximum revolution angle.

3 Analysis of Interlock Behavior under Load

3.1 Elasticity Calculation by Finite Elements Method

3.1.1 Method of Calculation

In order to obtain the optimum interlock shape

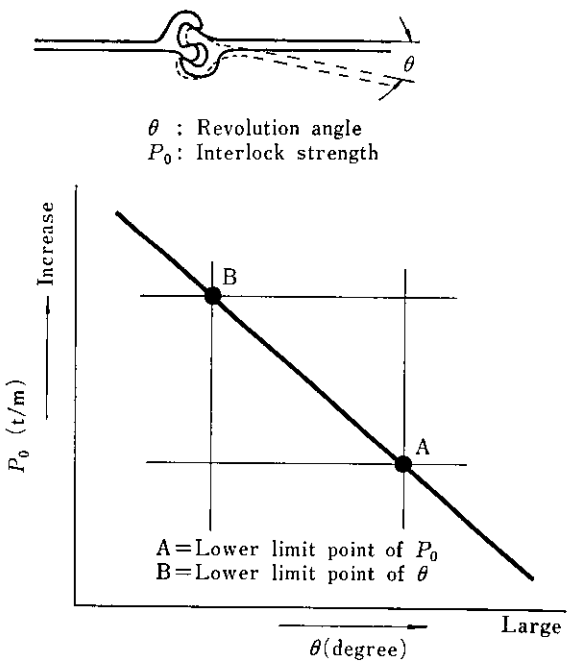

Fig. 1 Relation between θ and P_0

of FA flat-type steel sheet piling, stress and strain at various parts of interlocks of F flat-type steel sheet pilings combined and subjected to tensile force were calculated through the finite elements method (F.E.M.). It was assumed that contact points of combined interlocks did not move after loading.

3.1.2 Stress distribution

(1) Main stress for interlock elements
Main stress of elements constituting the interlocks of F-type sheet piling is illustrated in **Fig. 2**, and main stress values at contact points of combined interlocks, and at maximum stress points on thumbs and fingers are listed in **Table 1**. In both thumb and finger, the maximum tensile stress occurs at the inside of the minimum thickness section, which is regarded as critical area. All the contact points of interlocks are subjected to compressive stress, with compressive stress higher at the contact point between two thumbs (elements Nos. 473 and 539) than between a thumb and a finger (elements Nos. 452 and 534).

(2) Stress distribution in axial direction of web
The stress distribution in the axial direction of web at the minimum thickness section of thumb and finger is shown in **Fig. 3**. In both thumb and finger, the maximum stress values are nearly 30 kg/mm². In the thumb section (a–b section), the tensile state prevails as a whole, and the tensile stress in the axial direction of web dominates over the bending stress. On the other hand, in the minimum thickness section of finger (c–d section), the inside is subjected to tensile stress, and the outside to compressive stress, the bending stress dominating over the tensile stress in the axial direction of web.

3.1.3 Bearing ratio of web axial force

The web axial force components supported by

Table 1 Main stress at each position in interlocks of F-type sheet piling calculated by F.E.M.

	Number of elements	Main stress (kg/mm²)	Schematic view of interlocks
Finger	452	−21.1	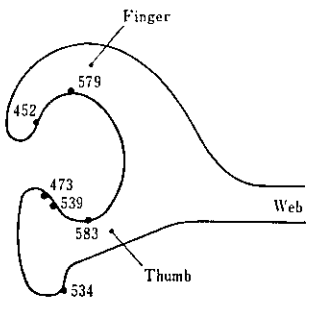
	579	+27.2	
Thumb	473	−24.6	
	534	−23.2	
	539	−26.5	
	583	+28.1	

452, 534: Point where thumb contacts finger
473, 539: Point where thumb contacts thumb
579 : Inside of critical section of finger
583 : Inside of critical section of thumb

Note (1) Axial force is 150 t/m
(2) Minus sign of main stress shows compression stress

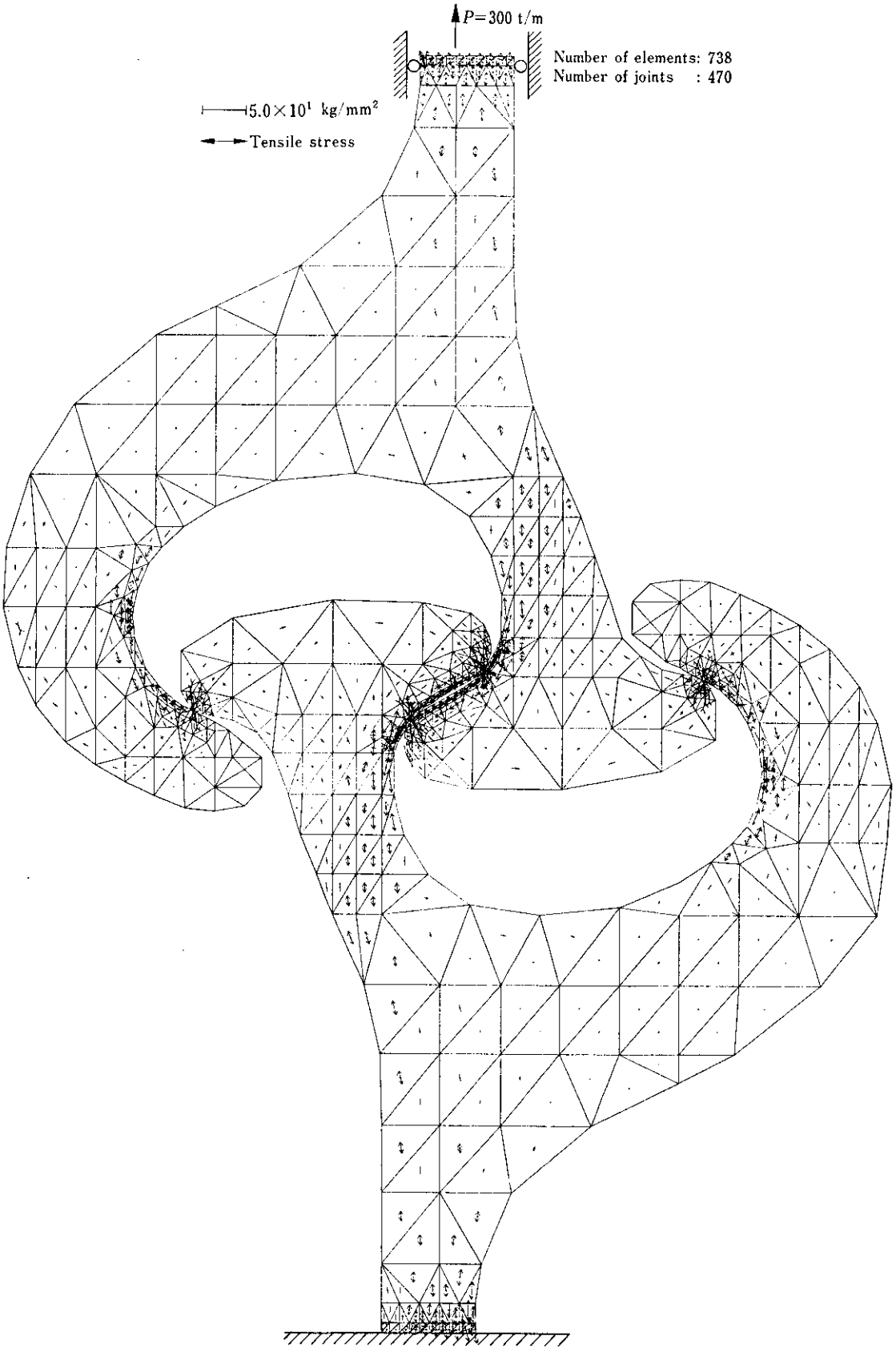

Fig. 2 View of element division and distribution of main stress of F-type sheet piling calculated by F.E.M.

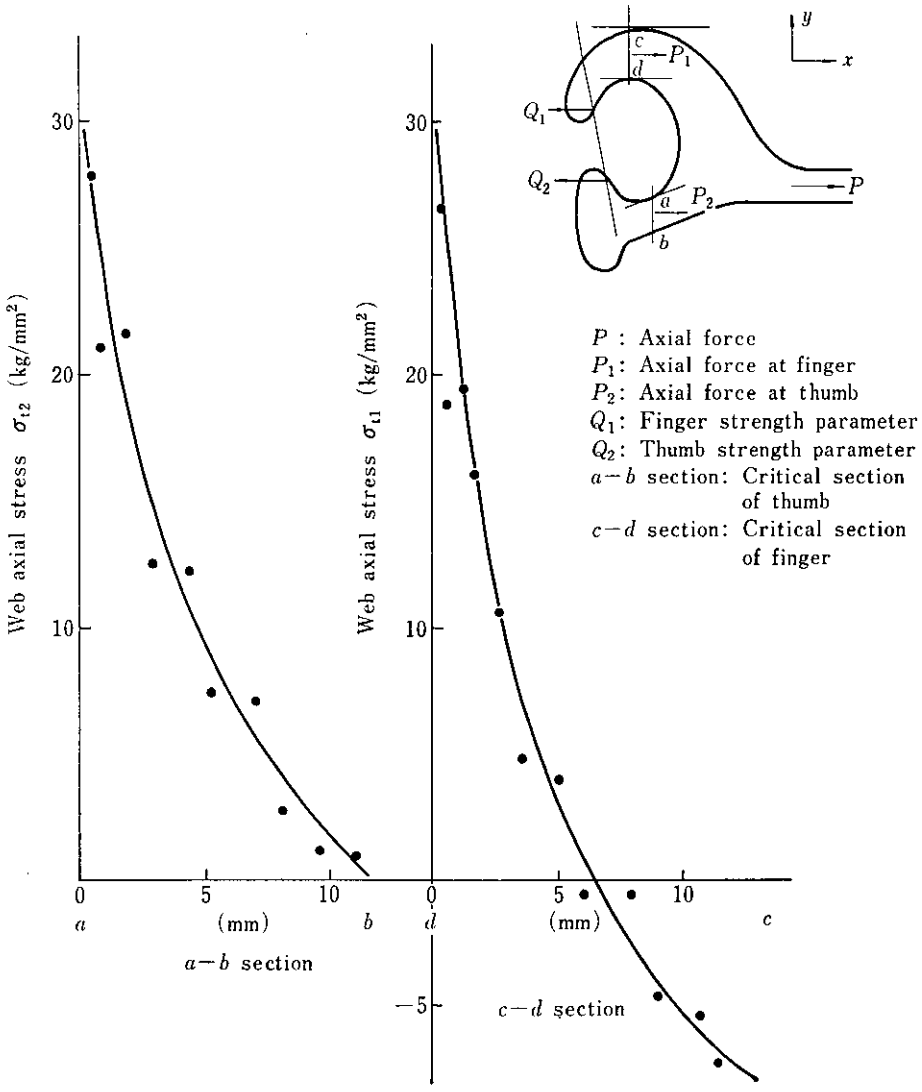

Fig. 3 Distribution of web axial stress at critical sections of F-type sheet piling when axial force is 150 t/m

thumb and finger are determined by integrating the stress distribution in the direction of web obtained in **Fig. 3**. Equation (1) applies to finger, (2) to thumb and (3) to the equilibrium with web axial force.
Web axial force of finger:

$$P_1 = \int_d^c \sigma_{t1}(y) \cdot dy \quad \cdots\cdots (1)$$

Web axial force of thumb:

$$P_2 = \int_b^a \sigma_{t2}(y) \cdot dy \quad \cdots\cdots (2)$$

Web axial force

$$P = P_1 + P_2 \quad \cdots\cdots (3)$$

$\sigma_{t1}(y)$: Web stress at minimum thickness section of finger
$\sigma_{t2}(y)$: Web stress at minimum thickness section of thumb

According to the calculation for loading 150 t/m web axial force, $P_1 = 37.5$ t/m and $P_2 = 112.5$ t/m. Hence, 1/4 of web axial force is supported by finger and 3/4 by thumb.

3.2 Interlock Tensile Test

3.2.1 Purpose of test

The deformation behavior of various parts of interlock under the web axial force was measured with F-type, as-rolled sheet piling. The results of inter-

lock tensile test were compared with the results of F.E.M. analysis described in the preceding section, to ascertain the reliability of calculation.

3.2.2 Testing method

The interlock tensile test was conducted on the basis of procedures specified in the Japanese Industrial Standards (JIS A 5528–1967). Deformations of interlock under load were measured at positions shown in **Fig. 4**. For the test, 30 t Amsler testing machine, contact type strain gauge (mark distance: 40 mm) and test-piece of F-type, as-rolled steel (50 mm width × 300 mm length) were used.

3.2.3 Test results

The test results are shown in **Fig. 5**. The deformation behavior of various parts of interlock is summarized as follows:

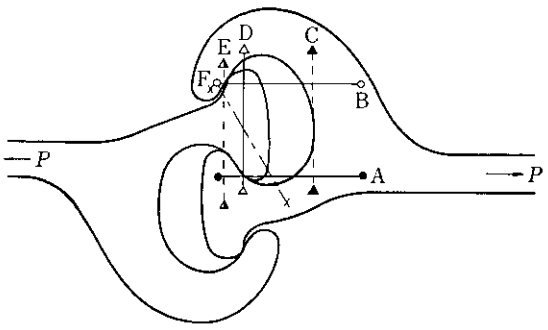

A: Web axis direction on thumb
B: Web axis direction on finger
C: Transverse direction at the root of thumb and finger
D, E, F: Transverse direction between thumb and finger

Fig. 4 Measured positions of deformation at interlocks of F-type sheet piling

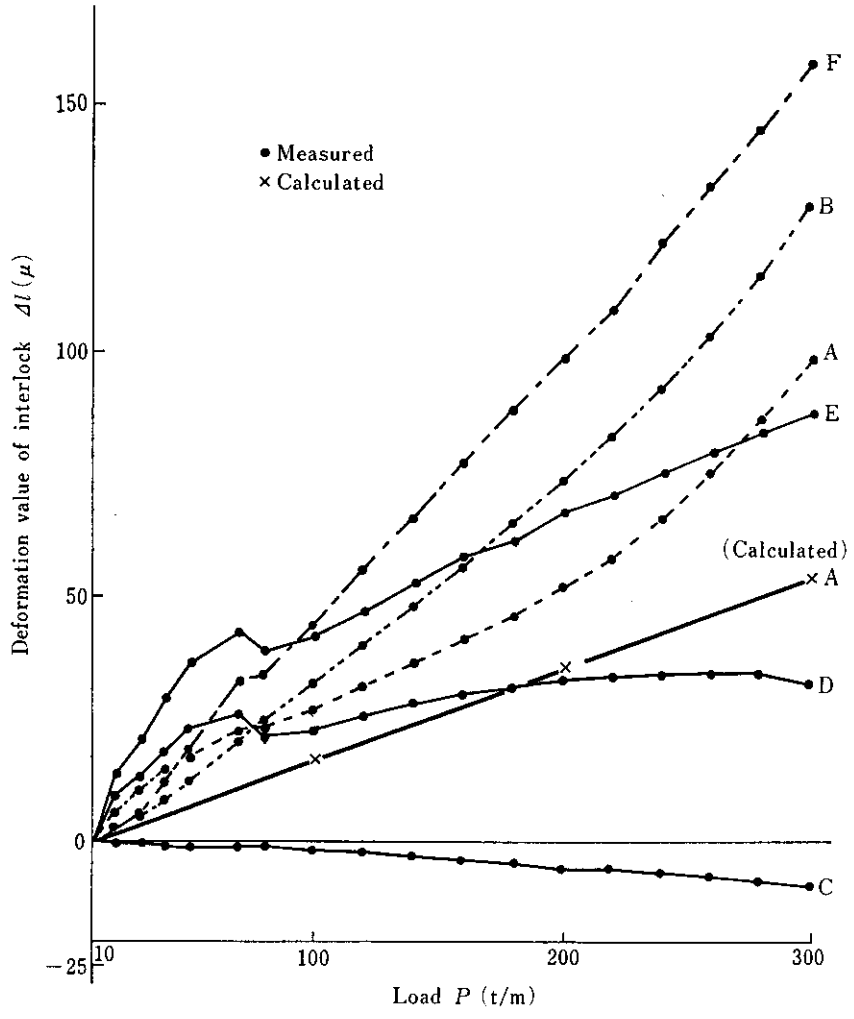

Fig. 5 Deformation values measured at each position shown in Fig. 4 and calculated at position A

(1) At the thumb (measuring points A and D), elongation in the web direction was dominant, while that in the normal direction to web due to bending was minor.
(2) At the finger (measuring points B, D, E and F), bending deformation to open finger was dominant, and accordingly, deformations in the web and normal directions were sizable. The bending deformation had its origin at the position of minimum thickness section. Hence, the deformation in the normal direction of web at point D was minimal.
(3) The root of thumb and finger (measuring point C) was affected by compressive strain due to elongation of thumb and bending deformation of finger, and the compressive deformation in the normal direction of web increased slightly as the load was increased.
(4) At contact points between thumbs and fingers, deformation grew faster in the load range of 0 to 80 t/m than in the range of 80 t/m or greater. This may be attributed to a slip generated at each contact point in the direction of stabilizing interlocking, immediately after the start of loading.

In the subsequent load range, the shifting of contact points stops, with deformation at various points limited only to that of elastic deformation of material. In consideration of large elongation at points B, E and F, representing outward bending of finger, it is evident that opening deformation of finger is largely responsible for unlocking of interlocks. In order to reduce finger deformation, it is necessary to design the shape of interlock so as to decrease the component of web axial force supported by the finger and to lower the bending moment acting upon the finger. Such a shape is considered to being about an improvement in the interlock strength.

3.3 Comparison with Elasticity Calculation

In **Fig. 6**, deformations of various portions of interlock per unit load up to max. 300 t/m are compared

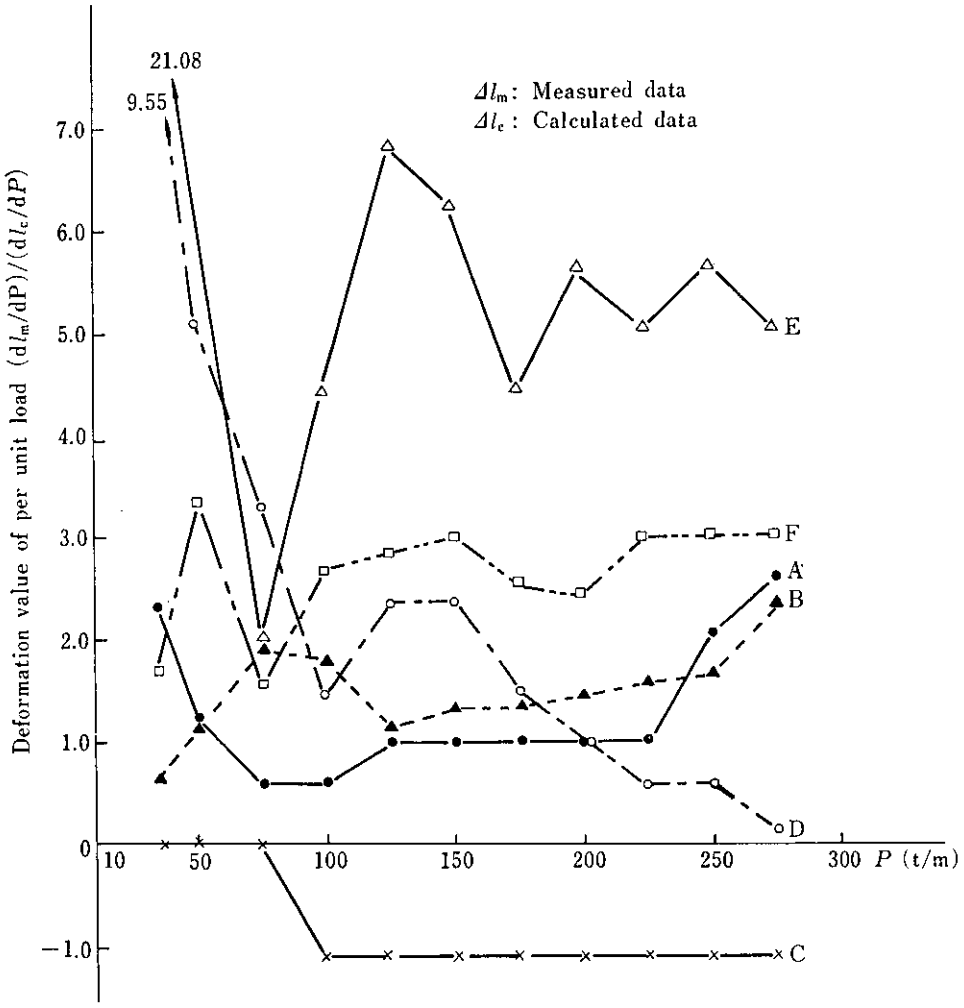

Fig. 6 Comparison of calculated data with measured data on defomation value of interlock at each position shown in Fig. 4

between the elasticity calculation using F.E.M. and actual measurements of tensile tests using as-rolled materials. Calculated values coincide with measured values if the ratio of deformation per unit load $d\,l_m/d\,l_c = \pm 1.0$. It is evident that measuring points A, B and C provide better approximation, and the F.E.M. results can be used for the displacement caused by the web axial force acting upon thumb and finger.

4 Analysis of Interlock Strength

4.1 Interlock Strength Coefficients

With regard to the effect of interlock shape on its strength, Bower[3], Neal[4] and Vasarhelyi[5] reported respective results based on the assumption that separation of combined interlocks occurred when the critical sections of both thumb and finger attained a fully plastic state. In these studies, the bearing ratio of web axial force between thumb and finger was ignored, and the interlock strength was determined as a sum of web axial force components which brought the respective critical sections of thumb and finger to the fully plastic range independently. The interlock strength values thus obtained are always greater than the actual ones. On the other hand, in the present study, it was assumed that separation depended upon the bending deformation of finger, and the web axial force to bring the critical section of finger to the fully plastic region was evaluated by considering bearing ratio of web axial force between thumb and finger.

So as to improve the accuracy of estimation. In order to facilitate the estimation of separation strength, interlock strength coefficient as defined by geometrical parameters of interlocks shown in **Fig. 7** was obtained.

Symbols to be used in the subsequent analysis are listed in the Appendix.

When sheet pilings rotate by angle β from the preloading state under the action of P with web thickness centers aligned, geometrical parameters are related with one another as shown by equations **(4)–(11)**.

$$a = (a_0 - e_0 \cdot \tan\beta) \cdot \cos\beta \quad \cdots\cdots\cdots (4)$$

$$b = (b_0 - i_0 \cdot \tan\beta) \cdot \cos\beta \quad \cdots\cdots\cdots (5)$$

$$c = a - b \quad \cdots\cdots\cdots (6)$$

$$d = (d_0 - y_0 \cdot \tan\beta) \cdot \cos\beta \quad \cdots\cdots\cdots (7)$$

$$y = (y_0 + d_0 \cdot \tan\beta) \cdot \cos\beta \quad \cdots\cdots\cdots (8)$$

$$\delta = \{\delta_0 + (a_0 + b_0 + y_0) \cdot \tan\beta\} \cdot \cos\beta \quad \cdots\cdots\cdots (9)$$

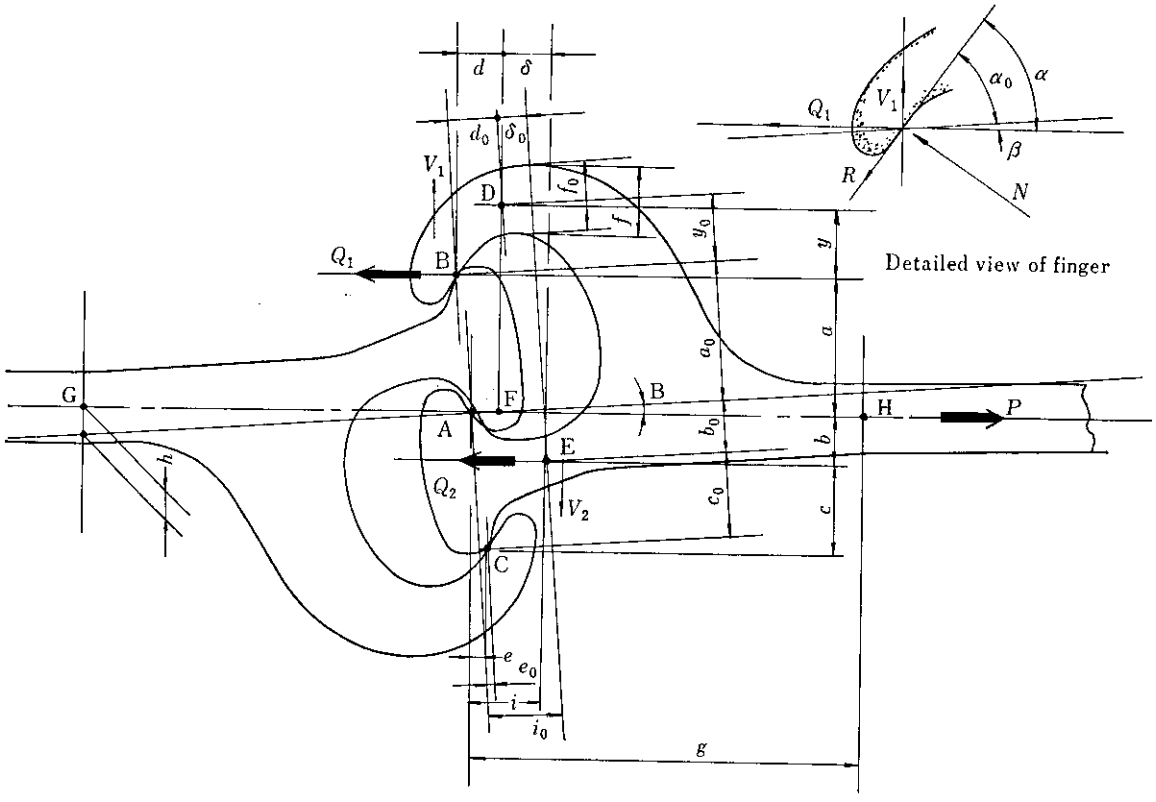

Fig. 7 Schematic view of geometical properties of interlocks

$$\beta = \tan^{-1}\frac{h}{g} \quad \cdots\cdots(10)$$

$$\alpha = \alpha_0 + \beta \quad \cdots\cdots(11)$$

From the equilibrium relations of forces in and normal to the web axial direction and moments around point F in **Fig. 7**

$$P = Q_1 + Q_2 \quad \cdots\cdots(12)$$

$$V_1 = V_2 \quad \cdots\cdots(13)$$

$$V_1 \cdot d - Q_1 \cdot a + V_2 \cdot \delta + Q_2 \cdot b = 0 \quad \cdots(14)$$

From the equilibrium relations at thumb-finger contact B,

$$Q_1 = N \cdot \sin\alpha + R \cdot \cos\alpha \quad \cdots\cdots(15)$$

$$R = \mu \cdot N \quad \cdots\cdots(16)$$

$$V_1 = N \cdot \cos\alpha - R \cdot \sin\alpha \quad \cdots\cdots(17)$$

Rearranging **(17)** with **(15)** and **(16)**, we obtain **(18)**.

$$V_1 = Q_1 \cdot \epsilon \quad \cdots\cdots(18)$$

where $\epsilon = 1 - \mu \cdot \tan\alpha / \mu + \tan\alpha$.
Q_1 and Q_2 can be calculated from **(6)**, **(12)**, **(13)**, **(14)** and **(18)**.

$$Q_1 = \frac{a - c}{(2a - c) - \epsilon(d + \delta)} \cdot P \quad \cdots\cdots(19)$$

$$Q_2 = \frac{a - \epsilon(d + \delta)}{(2a - c) - \epsilon(d + \delta)} \cdot P \quad \cdots\cdots(20)$$

Bending moment M acting upon the critical section of finger is given by **(21)** using shearing force and axial force. Assuming that the finger is a perfect elastoplastic body, and that shearing force, axial force and bending moment act upon the critical section of finger all at once, full-plastic state equations for beam **(22)**–**(25)** are applied. P_0 corresponding to the full-plastic state is the interlock separation strength.

$$M = Q_1 \cdot y + V_1 \cdot d = Q_1(y + \epsilon \cdot d) \quad \cdots(21)$$

$$\left(\frac{Q}{Q_P}\right)^2 + \left(\frac{V}{V_P}\right)^2 + \left(\frac{M}{M_P}\right) = 1 \quad \cdots\cdots(22)$$

$$Q_P = t \cdot f_0 \cdot Y \quad \cdots\cdots(23)$$

$$V_P = t \cdot f_0 \cdot Y/\sqrt{3} \quad \cdots\cdots(24)$$

$$M_P = t \cdot f_0^2 \cdot Y/4 \quad \cdots\cdots(25)$$

t: Beam width
Y: Yield stress
Q_P: Axial force for full-plastic state
V_P: Shearing force for full-plastic state
M_P: Bending moment for full-plastic state

Putting **(18)**, **(19)** and **(21)** into **(22)**, web axial force Q_1 acting upon finger is solved.

$$Q_1 = \left[\frac{-2(y + \epsilon \cdot d) + \sqrt{4(y + \epsilon \cdot d)^2 + (1 + 3\epsilon^2)f^2}}{(1 + 3\epsilon^2)}\right] \times t \cdot Y \quad \cdots\cdots(26)$$

Eliminating Q_1 for **(19)** and **(26)**, the interlock separation strength P_0 is given by **(27)**.

$$P_0 = \frac{P}{t} = \left[\frac{(2a - c) - \epsilon(d + \delta)}{(a - c)} \times \frac{-2(y + \epsilon \cdot d) + \sqrt{4(y + \epsilon \cdot d)^2 + (1 + 3\epsilon^2) \cdot f^2}}{(1 + 3\epsilon^2)}\right] \times Y = K \cdot Y \quad \cdots\cdots(27)$$

Equation **(27)** means that P_0 is determined by the yield stress of material and geometrical parameters of linked interlocks. The terms other than yield stress are defined collectively as interlock strength coefficient (K). While P_0 increases with K, the web axial force Q_1 acting upon thumb-finger contact decreases.

Q_1 for F type piling with standard dimensions is calculated from **(19)** as $Q_1 = 0.25\,P$. This agrees with the result obtained in the preceding paragraph (3.1.3), confirming the validity of **(19)**.

4.2 Relationship of *K*-Value to Interlock Strength

Geometrical parameters involved in K were measured in accordance with **Fig. 7** for interlocks of F-type as-rolled pilings of identical specification (SY 30), of which interlock separation strengths P_{0m} could be determined by the interlock tensile test, and these parameters were introduced into equation **(27)** to calculate K.

The relationship of K to P_{0m} is illustrated in **Fig. 8**,

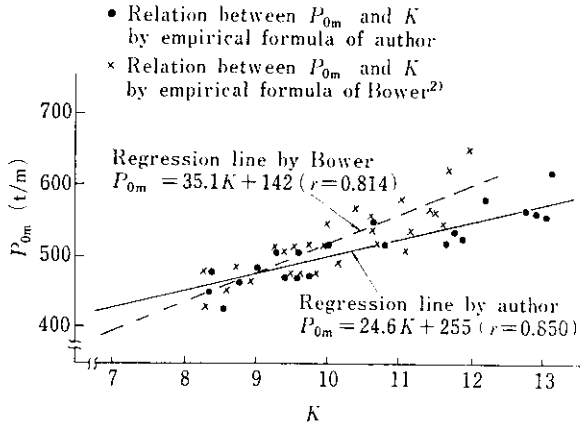

Fig. 8 Relation between coefficient of separation strength K and separation strength P_{0m} for rolled F-type sheet piling (Specification: SY 30)

where K values calculated with equations of Bower et al. are also plotted. There was a high positive correlation between K and P_{0m}, allowing to evaluate the interlock strength P_0 from K which can be calculated on the basis of interlock geometry and dimensions.

4.3 Effects of Various Interlock Parameters to Strength

Effects on K of individually changing various geometric parameters of interlock included in the fundamental equation **(27)** were calculated on the basis of standard dimensions of F-type piling. The results are shown in **Fig. 9**.

It is evident from **Fig. 9** that the larger f_0 is, the higher K becomes. However, it should be noted that increase of f_0 results in increase of weight.

Vertical geometric parameters of linked interlocks, c_0, a_0, y_0 and h exert marked effects: the greater c_0 and h are, and the smaller a_0 and y_0 are, the higher K becomes. This means that Q_1, supported by finger can be reduced so as to increase K by effectively changing c_0, a_0, y_0 and h. Additionally, another finger shape factor α_0 may be expected to contribute nearly the same effect as h. It is advantageous to increase μ for reducing the axial force, shearing force and bending moment acting upon thumb-to-finger contact B or C.

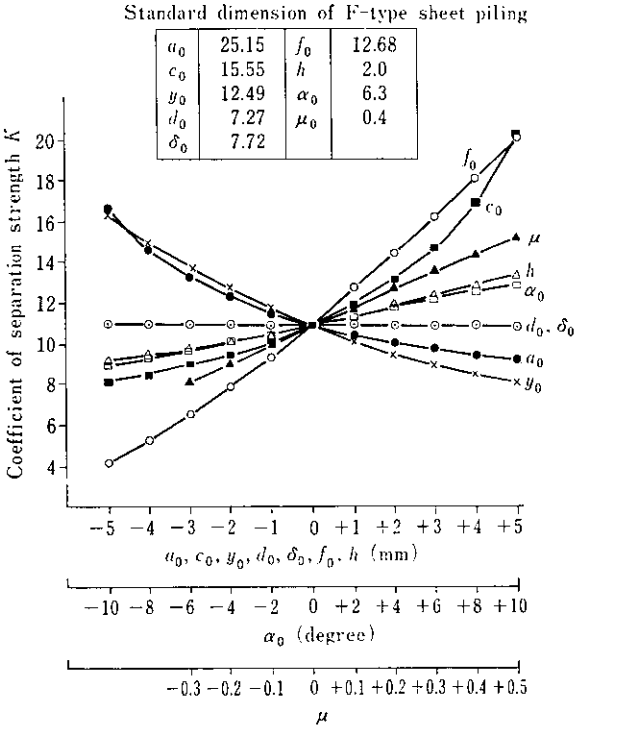

Fig. 9 Effect of interlocks parameter on separation strength

5 Design of Interlock Shape for FA-Type Piling

5.1 Effects of Interlock Dimensions

5.1.1 Evaluation by calculation

(1) Method of calculation

As described in the preceding section, it is necessary to increase K to obtain a higher P_0. In case of newly designing the interlock shape for FA type piling, however, it is impossible to specify the shape immediately because dimensions for linked interlocks mentioned in the preceding section were given in reference to load points of interlocks. For this reason, some shapes of interlock with modi-

Table 2 Details for change of geometical properties of interlock

Case No.	Dimension for design of interlock shape: Main factor	Dependent factor	Fixed factor	Dimension to be changed shown in Fig. 7
1	q_0	—	All factors except q_0	a_0, c_0, y_0, d_0, δ_0
2	q_0	j_0, r_0, ξ_0	k_0, m_0, n_0	a_0, c_0, y_0, d_0
3	q_0	j_0, m_0, n_0	k_0, r_0, ξ_0	a_0, c_0, y_0, d_0
4	m_0	r_0	All factors except r_0	a_0, c_0, y_0, d_0, δ_0
5	n_0	ξ_0	All factors except ξ_0	a_0, c_0, y_0, d_0, δ_0
6	k_0	n_0	All factors except n_0	a_0, c_0, y_0, d_0, δ_0
7	f_0	—	All factors except f_0	f_0
8	a_0	—	All factors except a_0	a_0
9	h	—	All factors except h	h, β
10	q_0, j_0, m_0, n_0	—	—	a_0, c_0, y_0, d_0, δ_0

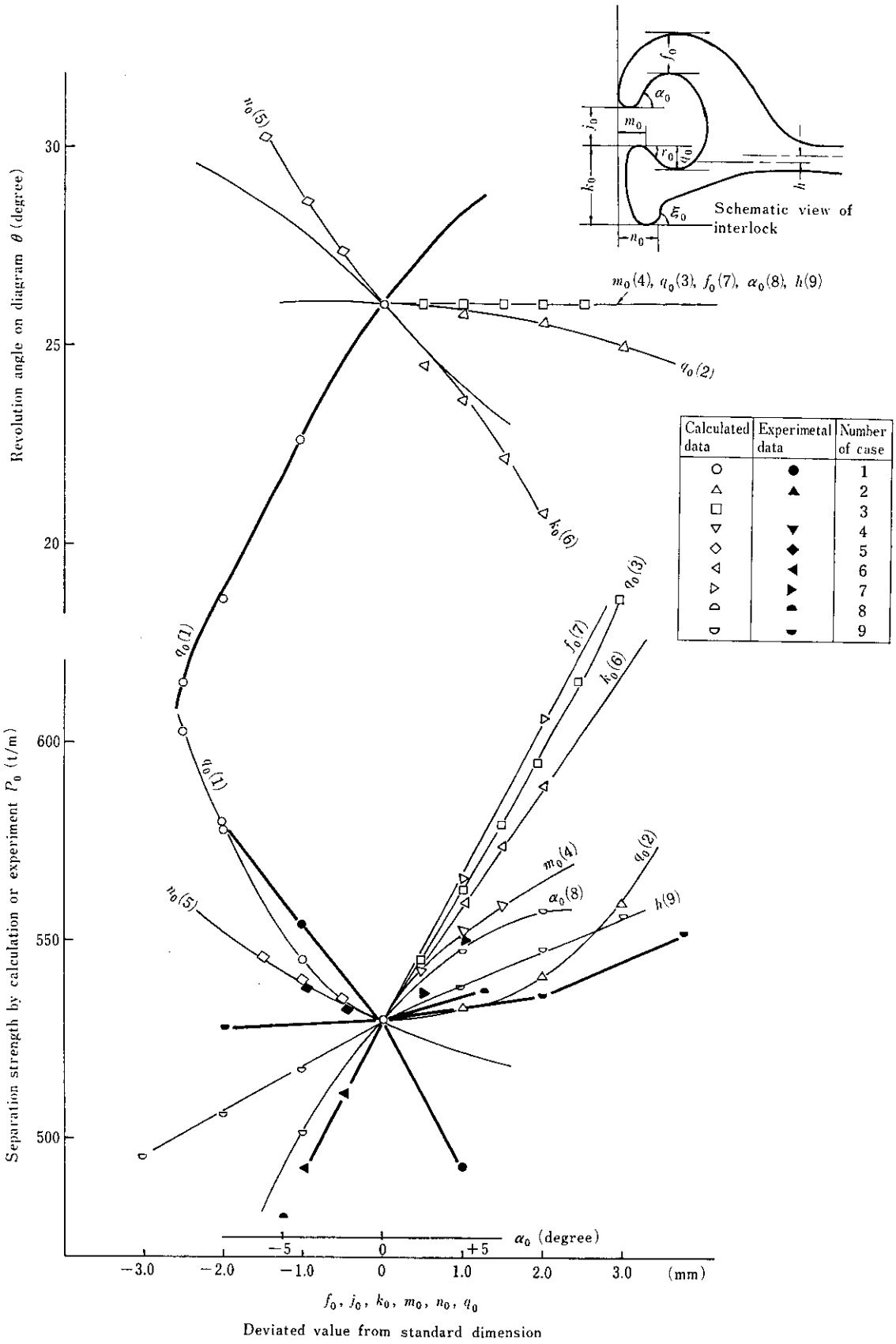

Fig. 10 Comparison between experimental and calculated data of separation strength and revolution angle with the change of f_0, j_0, k_0, m_0, n_0, and q_0

fied dimensions were drawn on 5/1 scale, and converted into the representation shown in **Fig. 7**, so as to calculate K from equation **(27)**. In this case, the maximum revolution angle was also measured. Modified dimensions of interlock are given in **Table 2**. K values for respective cases were introduced into the regression formula obtained in **Fig. 8** to estimate P_0.

(2) Results of calculation

Effects of various geometrical parameters (q_0, j_0, k_0, m_0, n_0, f_0, α_0 and h) to the interlock separation strength P_0 and the maximum revolution angle θ are shown in **Fig. 10**. Paying particular attention to dimensions n_0 and q_0 which effectively improve the interlock separations strength without affecting the maximum revolution angle, the relationship of interlock separation strength P_0 to the maximum revolution angle θ is shown in **Fig. 11**. From the results shown in **Figs. 10** and **11**, it is evident that three parameters n_0, m_0 and q_0 effectively contribute to improving P_0 without reducing θ. In Case No. 5, the smaller n_0 is, the greater both P_0 and θ become, while in Case No. 4, the greater m_0 is, the greater P_0 becomes, without affecting θ. If q_0 is changed with j_0 and k_0 fixed at values in Case No. 1 and the position of thumb critical section center is shifted vertically, the smaller q_0 is and the greater P_0 becomes, but θ is reduced extensively, giving an unfavorable result. However, in Cases Nos. 2 and 3, where q_0 is changed with k_0 and the position of thumb section center is fixed and j_0 variable, P_0 can be increased extensively with θ being affected only marginally. Particularly, when j_0 is changed with m_0 and n_0 fixed at values in Case No. 3, P_0 is increased markedly. To sum up, changes in dimensional parameters as described below give favorable results in designing an interlock shape with greater P_0.

(a) To reduce n_0.

(b) To increase m_0.

(c) To reduce q_0 by changing m_0 and n_0 with k_0 fixed.

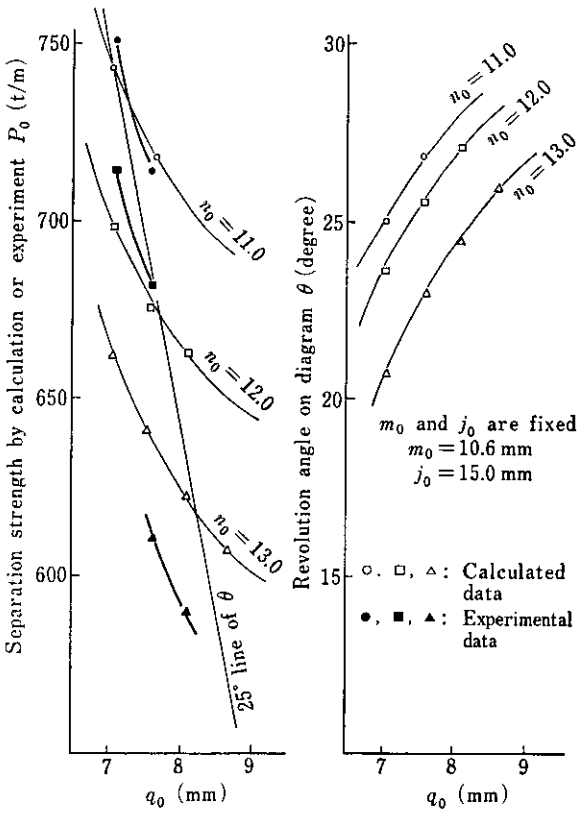

Fig. 11 Comparison between experimental and calculated data of separation strength and revolution angle with the change of n_0 and q_0 (by case 10)

5.1.2 Checking by interlock tensile test

(1) Testing method

In order to ascertain the results of calculation described in the preceding section, specimens having interlock shapes corresponding to cases mentioned in **Table 2** were manufactured by machining for the interlock tensile test. (These specimens are referred to as models hereinafter.) Chemical composition and mechanical properties of specimens are given in **Table 3**. Because of the capability of the machine-tool to manufacture models, the width

Table 3 Chemical composition and mechanical properties of specimens by machinery processing

Specification	Thickness (mm)	Heat treatment	Chemical composition					Mechanical properties (tensile test)		
			C	Si	Mn	P	S	Y.P.	T.S.	El.
SM 50A	22.0	Normalizing	0.16	0.32	1.35	0.017	0.008	34.5	53.5	30

Y.P.: Yield stress (kg/mm²)
T.S.: Tensile strength (kg/mm²)
El. Elongation (%)

Table 4 Chemical composition and mechanical properties

Steel	Chemical composition (wt.%)								Mechanical properties (tensile test)		
	C	Si	Mn	P	S	Cu	Cr	V	Y. P.	T. S.	El.
SY 30	0.31	0.07	0.81	0.024	0.021	0.29			39.4	56.7	24
A	0.15	0.22	1.00	0.025	0.018	0.31	0.52	0.032	48.6	61.2	20

Y.P.: Yield stress (kg/mm^2)
T.S.: Tensile strength (kg/mm^2)
El. Elongation (%)

and length of a test-piece were set to 18.0 mm and 220 mm, respectively. In order to check the effects of shape and dimensions of interlock alone, the web thickness of model was fixed at 13.0 mm to avoid web rupture. The accuracy of model machining was 1/100–2/100 mm.

(2) The results

The results of model interlock tensile tests are included in **Figs. 10** and **11**. Though the results of model interlock tensile tests failed to coincide with the interlock strength P_0 calculated on the basis of interlock shape coefficient K_B because of the difference in material strength, and frictional coefficient at thumb-to-thumb and thumb-to-finger contacts, it was found that P_0 could be increased by changing the shape of thumb or finger in the F-type standard interlock. As for θ, there was no discrepancy between results of drawing and model experiment, which are not shown here.

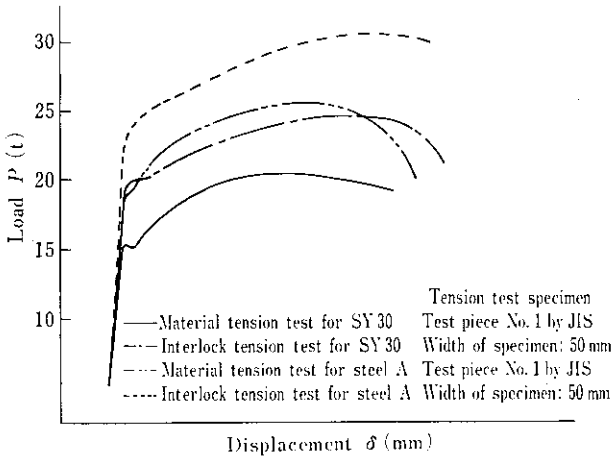

Fig. 12 Load-displacement curve to investigate the change of interlock strength by steel materials shown in Table 4

6 Effects of Materials Characteristics

6.1 Testing Method

Besides increasing K, P_0 can be made greater by increasing the other term of equation **(27)**, Y. In order to elucidate the effect of Y to P_0, characteristics of SY 30, material of commercially available steel sheet piling, and of high-tension steel (steel A) prepared for increasing Y were compared. Chemical composition and mechanical properties of materials tested are shown in **Table 4.**

6.2 Test Results

The load-displacement curves of SY 30 and steel A obtained by the material tensile test and interlock tensile test are shown in **Fig. 12.** The interlock tensile strength is extensively affected by yield load of the material. The load increments from yield load to maximum load are rather small and almost identical for two materials. The interlock tensile strength can, therefore, approximately be determined by the strength in elastic domain. Since the ratio of yield stress of SY 30 to that of steel A ($Y_A/Y_{SY\ 30} = 48.6/39.4 = 1.23$) is very close to the corresponding rato of interlock tensile strength ($P_{0A}/P_{0\ SY\ 30} = 30.5/24.5 = 1.24$), it is possible to estimate the improvement of interlock strength on the basis of increment in yield stress.

7 Conclusion

In order to determine the optimum shape of flat-type steel sheet piling interlock to increase P_0 without reducing θ, theoretical analysis and interlock tensile test were conducted, and the following results were obtained.

(1) Based on the assumption that linked interlocks are made at thumb-to-thumb and thumb-to-finger contacts, the result of elasticity calculation of the bearing ratio of web axial force between thumb

and finger by F.E.M. agreed with that of the interlock tensile test using as-rolled materials, except for a discrepancy due to slip at contact points immediately after starting loading.

(2) The maximum stress acting upon thumb and finger is located at the inside of minimum thickness section of thumb and finger.

(3) Stress conditions at the minimum thickness section of thumb and finger are such that in the thumb, the tensile stress due to web axial force is dominant over the bending stress, while in the finger the bending stress associated with opening is dominant over the tensile stress.

(4) With regard to interlock deformation, the bending deformation of finger was greatest.

(5) K, calculated on the assumption that the interlock separation strength depends upon the bending deformation of finger, was determined by the interlock shape and μ at thumb-to-thumb and thumb-to-finger contacts of linked interlocks. There was a high positive correlation between K and interlock separation strength.

(6) K could be increased by reducing Q_1.

(7) The optimum interlock shape for increasing P_0 while minimizing the reduction of θ and the increase of weight could be attained by increasing m_0 and h, and decreasing q_0 and n_0.

(8) In the case of identical interlock shape, P_0 could be further increased by increasing the yield strength of materials and the coefficient of friction at thumb-to-thumb and thumb-to-finger contacts of interlocks.

On the basis of these results, we completed the development of the FA type flat steel sheet piling, aiming at interlock strength of 700 t/m. Our aim is to manufacture flat steel sheet piling having stable interlock strength through the improvement of rolling accuracy and product quality.

Appendix: List of symbols used in the equations **(4)–(27)**

a, a_0: Vertical distance from thumb-to-thumb contact A to thumb-to-finger contact B

b, b_0: Vertical distance from thumb-to-thumb contact A to the center of thumb minimum thickness section

c, c_0: Vertical distance from thumb-to-finger contact B or C to the center of thumb minimum thickness section

y, y_0: Vertical distance from thumb-to-finger contact B or C to the center of finger minimum thickness section

d, d_0: Horizontal distance from thumb-to-finger contact B or C to the center of finger minimum thickness section

δ, δ_0: Horizontal distance from the center of finger minimum thickness section to the center of thumb minimum thickness section

h: Deviation between centers of interlocked web thickness before loading

i, i_0: Horizontal distance from thumb-to-thumb contact A to thumb minimum thickness section

e, e_0: Horizontal distance from thumb-to-thumb contact A to thumb-to-finger contact B or C

α, α_0: Angle between finger inside and web axis at B or C

f, f_0: Thickness of finger at minimum thickness section ($f \fallingdotseq f_0$)

g: Horizontal distance from thumb-to-thumb contact A to a given point G or H on the line of action of web axial force passing through A

β: Revolution angle corresponding to h for stabilizing interlocking after starting loading

μ: Coefficient of friction

P: Web axial force

Q_1: Web axial force acting upon thumb-finger contact

Q_2: Web axial force acting upon thumb

V: Shearing force

V_1: Shearing force acting upon thumb-finger contact B or C

V_2: Shearing force acting upon thumb

R: Tangential force of finger

N: Vertical force acting upon finger tangent

$a_0, b_0, c_0, \cdots$: Geometric parameters for linked interlocks before starting loading

$a, b, c, \cdots$: Geometric parameters for interlocks subjected to revolution by angle β after starting loading

References

1) T. Ishiwata: *Kowan* **53** (1976) 8, pp. 61–71
2) M. Ishida, Y. Kawai, I. Jo and H. Nakagawa: *Kawasaki Steel Technical Report*, **11** (1979) 4, pp. 111–125 (in Japanese)
3) J.E. Bower: Proc. ASCE; *Journal of the Socil Mechanics & Foundation Division*, **99**(Oct., 1973) No. SM10, p. 765
4) G. Neal: *Journal of Applied Mechanics* (1961) Jun., p. 269
5) D.V. Vasarhely: Proc. ASCE, *Journal of The Structural Division*, **93**(Aug., 1967) No. ST8, pp. 227–235